Bioorganic & Medicinal Chemistry Letters 19 (2009) 5665–5669

Contents lists available at ScienceDirect

Bioorganic & Medicinal Chemistry Letters

journal homepage: www.elsevier.com/locate/bmcl

The first pharmacophore model for potent NF-κB inhibitors

Keng-Chang Tsai [a,†], Li-Wei Teng [b,c,†], Yi-Ming Shao [a], Yu-Chen Chen [d], Yu-Ching Lee [a], Minyong Li [e], Nai-Wan Hsiao [b,*]

[a] Genomics Research Center, Academia Sinica, Taipei 11529, Taiwan
[b] Institute of Biotechnology, National Changhua University of Education, Changhua 50007, Taiwan
[c] Pharmaceutical R&D Laboratories, Department Center For Biotechnology, Taipei 22180, Taiwan
[d] Department of Biological Science and Technology, China Medical University, Taichung 40402, Taiwan
[e] Department of Medicinal Chemistry, School of Pharmacy, Shandong University, Jinan, Shandong 250012, China

ARTICLE INFO

Article history:
Received 24 March 2009
Revised 4 August 2009
Accepted 5 August 2009
Available online 8 August 2009

Keywords:
Pharmacophore
NF-κB inhibitor
CATALYST
QSAR

ABSTRACT

As an important transcription factor of the *Ral* family, nuclear factor-kappa B (NF-κB) is involved in numerous cellular processes, such as the responses to cellular stress and to inflammation. For better elucidating the quantitative structure–activity relationship of NF-κB inhibitors and determining possible ligand–protein interaction, a pharmacophore model, Hypo1, was built based on 35 training molecules by Catalyst/HypoGen algorithm. The five pharmacophore features of Hypo1, including three hydrophobic groups, one hydrogen-bond acceptor, and one hydrophobic aromatic group, were correctly mapped onto NF-κB surface. This model has strong capability to identify NF-κB inhibitors and to predict the activities of structurally diverse molecules, thus to provide a valuable tool in the design of new leads with desired biological activity by virtual screening.

Nuclear factor-kappa B (NF-κB) is a very important eukaryotic transcription factor for various immune and inflammatory responses. Normally existing as inactive form in the cytoplasm, NF-κB heterodimer composed of p50 and p65 (Rel A) subunits is inhibited by binding with IκB family proteins,[1–4] subsequently NF-κB nuclear translocation is blocked. NF-κB does not release and translocate into nucleus until outside signaling induces IκB degradation, phosphorylation, and polyubiquitination.[5–9] NF-κB functions in regulating the expression of normal immunologic responses, and NF-κB activation in response to pro-inflammatory stimuli such as tumor necrosis factor-α (TNF-α) and interleukin-1β (IL-1β), has been extensively characterized. However, excessive activation of NF-κB can lead to inflammatory disorders, such as bowel disease, psoriasis, asthma, rheumatoid arthritis, and sepsis.[10–12]

Current approaches for the treatment of inflammation mainly rely on inhibiting pro-inflammatory mediator production and quenching initial inflammatory response. For example, selective inhibitors of NF-κB activation are expected as the potent therapeutic agents for inflammatory diseases.[13–15] Previous reports disclosed diverse inhibitors of NF-κB activation, including MG-132[16] and indan derivatives.[17] In 2003, Tobe et al. reported a novel structural class of quinazoline derivatives as interesting NF-κB inhibitors. It needs to be emphasized that a few of potent NF-κB inhibitors exhibited anti-inflammatory effects on carrageenin-induced paw edema in vivo.[18,19] The evidences that these inhibitors showed awesome biological potential drive us to find their common structural moieties by using computational approach. Since pharmacophore modeling is among the most state-of-the-art component in a ligand-based molecular design, we herein employ the above-mentioned NF-κB inhibitors to identify their common features.

As the most leading algorithm for the automated generation of pharmacophore models and 3D database searching,[20] the HypoGen module in the CATALYST 4.11 package (Accelrys Inc.) was selected to identify the common features for NF-κB inhibitors.[21] It should be noted that this HypoGen algorithm has been demonstrated by a large number of successful applications in medicinal chemistry.[22–25] In our current study, considering the structural diversity and activity coverage, two molecule sets, including training and test sets, were collected for the development of pharmacophore model from the literatures.[16–19] The chemical structures of 35 training set compounds are presented in Figure 1. Biological activities against NF-κB are reported as IC_{50} values spanning from 2 nM to >10,000 nM with four orders of difference. All calculations were performed on Scorpio SGI Origin 3800 (NCHC, Taiwan). Firstly, each structure was energy-minimized using the CHARMM-like force field[26] within CATALYST 4.11 package and subjected to a

* Corresponding author. Tel.: +886 04 7232105 3421; fax: +886 4 7211156.
E-mail addresses: nady@cc.ncue.edu.tw, g874285@life.nthu.edu.tw (N.-W. Hsiao).
† Co-first author.

0960-894X/$ - see front matter © 2009 Elsevier Ltd. All rights reserved.
doi:10.1016/j.bmcl.2009.08.021

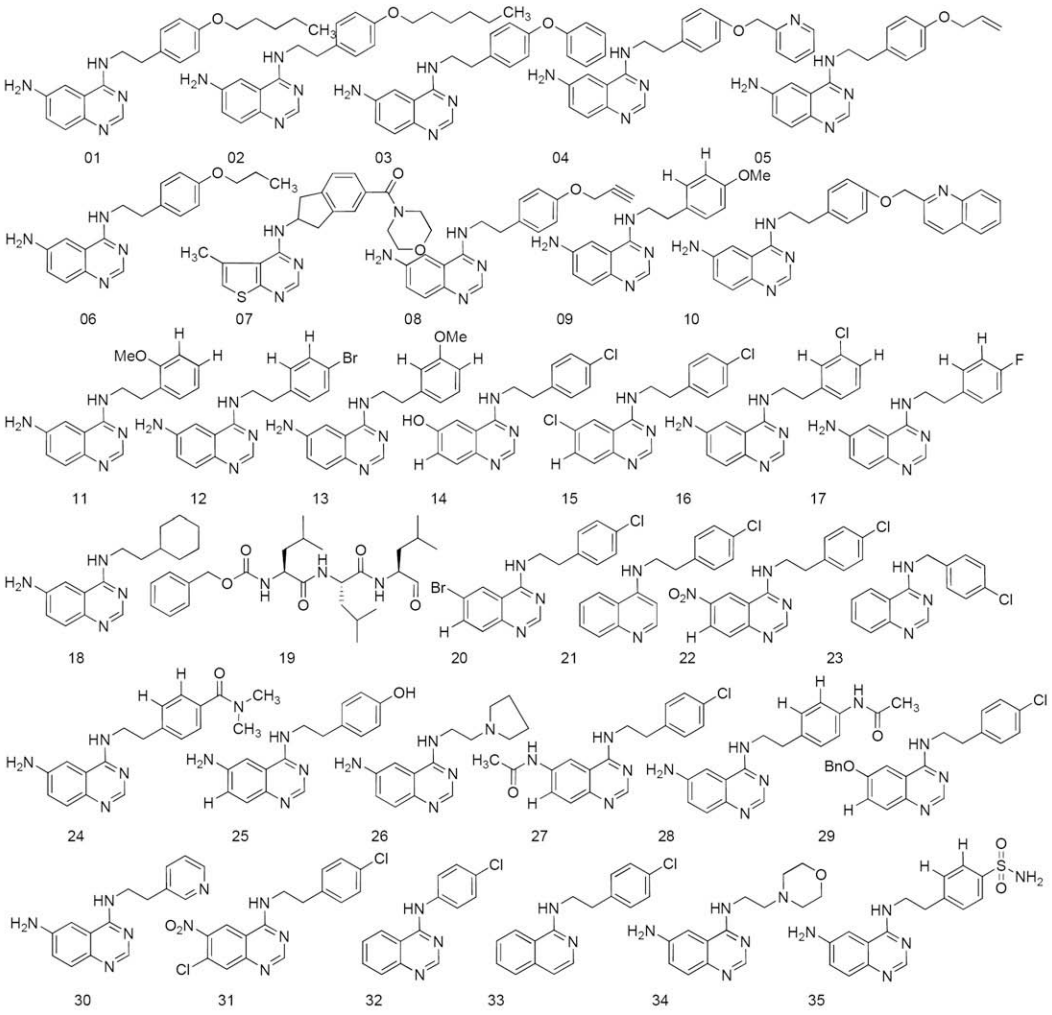

Figure 1. The chemical structures of all 35 training set molecules used for HypoGen pharmacophore generation.

conformational analysis using the Poling algorithm.[27] In this case, the maximum number of conformations allowed for each compound was set to 250 with 20 kcal/mol energy cutoff. All other parameters were default, except the Uncert value of 2.0. In addition, there is a 3.5 order of magnitude difference in activity relative to the active molecules, and this difference changed from 3.5 to 3.67 by modulating the parameter. Furthermore, in the hypothesis generation phase, three pharmacophore features: hydrogen-bond acceptor (HA), hydrophobic group (H), hydrophobic aromatic (HR), were considered by HypoGen. The HypoGen algorithm was forced to determine pharmacophore models that contain 1-3 HA and HR features, and 3-5 H features. Finally, the top 10 scoring hypotheses composed of these three pharmacophore features for each set were exported.

CATALYST produced 10 hypotheses, and all include five common features—one hydrogen-bond acceptor (HA), one hydrophobic aromatic (HR), and three hydrophobic group (H). Among these 10 hypotheses, Hypol is the most reasonable (Fig. 2) as characterized by its lowest total cost, highest cost difference (Δcost), lowest root-mean-square deviation, and best correlation coefficient. The HypoGen method performs two important theoretical cost calculations for determining the success of any pharmacophore hypothesis[28] (see Supplementary, Theoretical cost calculations for HypoGen). Statistically, the null cost value of the top 10 hypotheses of 324.455, the fixed cost value of 114.035, configuration cost value of 11.303, the highest cost difference between null and total cost of 170.186, and configuration cost value of 11.303 were obtained (see Supplementary data, Table S1). Furthermore, a high correlation coefficient of 0.909 (see Supplementary data, Fig. S1) as well as RMS deviation of 1.490 demonstrates that this pharmacophore is of statistical significance and can be considered as a reliable pharmacophore model for further study. In addition, the activities of 35 training set molecules were correctly predicted by the Hypo1 hypothesis as summarized in Table 1. The difference between experimental and estimated activity values is represented as error (ratio between the larger and the smaller). This difference may have a negative sign if the experimental value is higher than the estimated. In brief, except molecule **35**, all molecules were correctly predicted in their activity category. These results confirm again the accuracy of our pharmacophore model by predicting correctly at 97% successful rate.

The reliability of Hypo1 hypotheses was cross-validated by using the CatScramble module.[21] The purpose of this cross-validation is to randomize the activity data among the training set compounds and to generate pharmacophore model using the same features and parameters as developing the original Hypo1 hypotheses. To achieve a confidence level of 95% (significance = $[1 - (1 + 0)/(19 + 1)] \times 100\% = 95\%$), 19 random spreadsheets (random hypotheses) were generated, and the results are listed in Supplementary data, Table S2. All 19 resulting hypotheses after randomization exhibited worse

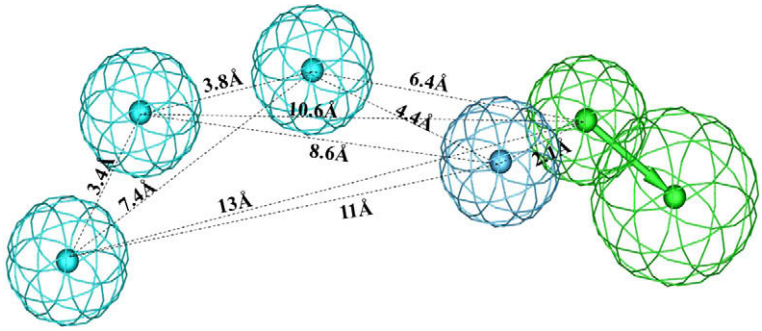

Figure 2. The best pharmacophore model Hypo1. Features are color-coded as follows: hydrophobic aromatic, blue; hydrogen-bond acceptor, green; hydrophobic, light blue.

Table 1
Experimental and estimated activity IC_{50} (nM) values of the training set molecules based on the pharmacophore model Hypo1

ID[a]	Actual IC_{50} (nM)	Category[b]	Estimated IC_{50} (nM)	Category[b]	Error	Ref.
1	2	+++	3.3	+++	+1.7	18
2	4	+++	5	+++	+1.3	18
3	11	+++	58	+++	+5.3	18
4	12	+++	23	+++	+1.9	18
5	12	+++	15	+++	+1.3	18
6	20	+++	41	+++	+2.1	18
7	38	+++	66	+++	+1.7	18
8	40	+++	35	+++	−1.1	18
9	90	+++	43	+++	−2.1	18
10	93	+++	44	+++	−2.1	18
11	155	++	280	++	+1.8	18
12	207	++	1400	++	+6.8	18
13	210	++	730	++	+3.5	18
14	313	++	460	++	+1.5	19
15	344	++	400	++	+1.2	19
16	389	++	410	++	+1.1	18
17	574	++	1200	++	+2.1	18
18	685	++	2400	++	+3.5	18
19	715	++	1100	++	+1.5	18
20	851	++	1400	++	+1.6	19
21	1392	++	1400	++	+1.0	19
22	1515	++	2100	++	+1.4	19
23	1832	++	1800	++	−1.0	19
24	2594	++	370	++	−7.0	18
25	3645	++	1400	++	−2.6	18
26	3694	++	1300	++	−2.8	18
27	4562	++	1200	++	−3.8	19
28	5979	++	1400	++	−4.3	18
29	7340	++	920	++	−8.0	19
30	8271	++	1600	++	−5.2	18
31	9060	++	2200	++	−4.1	19
32	>10,000	+	54,000	+	+5.4	19
33	>10,000	+	12,000	+	+1.2	19
34	>10,000	+	20,000	+	+2.0	18
35	>10,000	+	3100	++	−3.2	18

[a] Training set compound number.
[b] Categorical activity: IC_{50} > 10,000 nM '+'; 100 nM < IC_{50} < 10,000 nM '++'; IC_{50} < 100 nM '+++'.

performance than Hypo1. Thus, this cross-validation confirmed again the correlation of structures and experimental activities in the training sets, and provided us strong confidence on Hypo1.

The mapping of Hypo1 hypothesis onto two highly active inhibitors in the training set, compounds **1** (IC_{50} = 2 nM) and **2** (IC_{50} = 4 nM), yields a good fit with all features of the pharmacophore model Hypo1 (see Supplementary data, Fig. S2). The hydrogen-bond acceptor features (HA) were mapped onto the nitrogen at the quinazoline ring, the hydrophobic aromatic features (HR) were located onto the phenyl ring, and the three hydrophobic features (H) were existed onto the phenyl ring and the alkyl chain, respectively. In order to further validate our pharmacophore model Hypo1, a test set including external compounds **36–53** with different activity was analyzed (Fig. 3). The experimental and estimated activities and error values are shown in Table 2. In this test set validation, a correlation coefficient of 0.836 shows a good correlation between the experimental and estimated activities (see Supplementary data, Fig. S1). All test set compounds, except compound **53**, have no more than one order difference between estimated and experimental activity. In other words, test set compounds could be predicted correctly for their activity category with 94% successful rate.

However, most of these pharmacophores are based on quinazoline moiety. In order to enhance the predictability and accuracy of the model, we searched several structurally distinct inhibitors, namely, *N*-(quinolin-8-yl)benzenesulfonamides, thalidomide, and rocaglamide, as shown in compounds **54**–**92** (see Supplementary data, Fig. S3).[29–31] The representative compounds **54**, **60**, and **63**

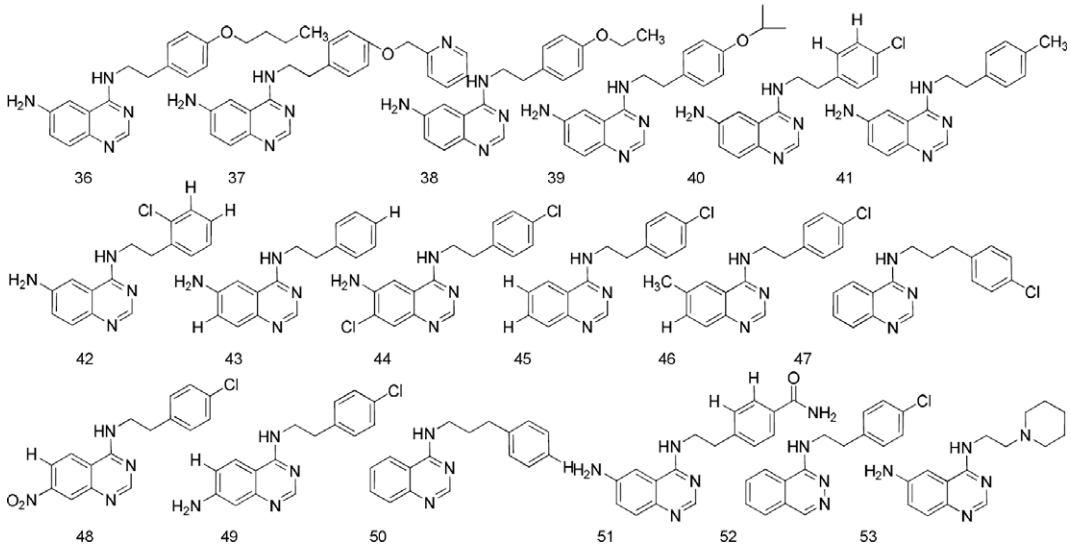

Figure 3. The chemical structures of all 18 test set molecules.

Table 2
Experimental and estimated IC_{50} (nM) values of the test set molecules based on the pharmacophore model Hypo1

ID[a]	Actual IC_{50} (nM)	Category[b]	Estimated IC_{50} (nM)	Category[b]	Error	Ref.
36	11	+++	10	+++	−1.1	18
37	14	+++	17	+++	+1.2	18
38	21	+++	27	+++	+1.3	18
39	40	+++	36	+++	−1.1	18
40	176	++	1300	++	+7.4	18
41	210	++	1500	++	+7.1	18
42	254	++	1300	++	+5.1	18
43	311	++	1600	++	+5.1	18
44	429	++	460	++	+1.1	19
45	630	++	1400	++	+2.2	19
46	730	++	1300	++	+1.8	19
47	1401	++	420	++	−3.3	19
48	1765	++	3300	++	+1.9	19
49	2202	++	1200	++	−1.8	19
50	2381	++	480	++	−5.0	19
51	7333	++	1600	++	−4.6	18
52	>10,000	+	45,000	+	+4.5	19
53	>10,000	+	1800	++	−5.6	18

[a] Test set compound number.
[b] Categorical activity: IC_{50} > 10,000 nM '+'; 100 nM < IC_{50} < 10,000 nM '++'; IC_{50} < 100 nM '+++'.

were mapped to the features of Hypo1 model (Fig. 4). We observed that rocaglamide group was mapped onto hydrophobic features (H) and hydrophobic aromatic features (HR), thalidomide group

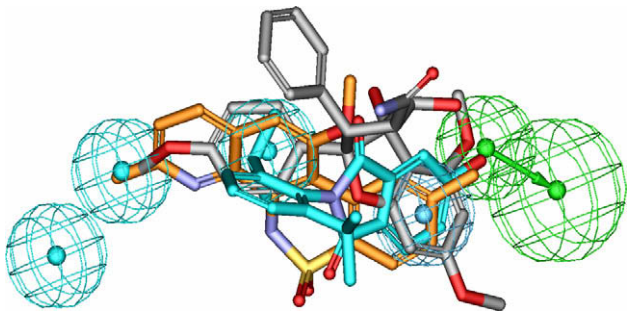

Figure 4. Mapping of the representative compounds **54** (gray color), **60** (light blue color), and **63** (orange color) onto Hypo1 hypothesis. Features are color-coded as follows: hydrophobic aromatic, blue; hydrogen-bond acceptor, green; hydrophobic, light blue.

was mapped onto hydrophobic aromatic features (HR), and *N*-(quinolin-8-yl) benzenesulfonamides groups were mapped onto hydrophobic features (H) and hydrophobic aromatic features (HR). In addition, as shown in Supplementary data, Table S3, the error values of all compounds were less than 10, and the estimated activities have high accuracy for their categorical activities with 94% successful rate. These results demonstrate that our model could be utilized to predict the activities of structurally diverse inhibitors accurately and thus can be a reliable ligand-based tool for the development of novel NF-κB inhibitors.

Previous reports[9,32–34] indicated that the NF-κB (p50–p65) structure bounds to κB site DNA, and the p50 subunit preferentially occupies the 5′ end of target DNA. The specific residues, including Arg356, Tyr357, Val358, Cys359, Glu360, Gly361, Pro362, Ser363, His364, Gly365, Gly366, Leu367, and Pro368, are involved in the interaction with the DNA.[35–38] For NF-κB, there are four pockets adjacent to DNA binding region. Therefore, we would like to identify which pocket Hypo1 favors by molecular docking using a genetic algorithm based program (GOLD).[39–41] In brief, the crystal structure of p50–p65 complex was obtained from

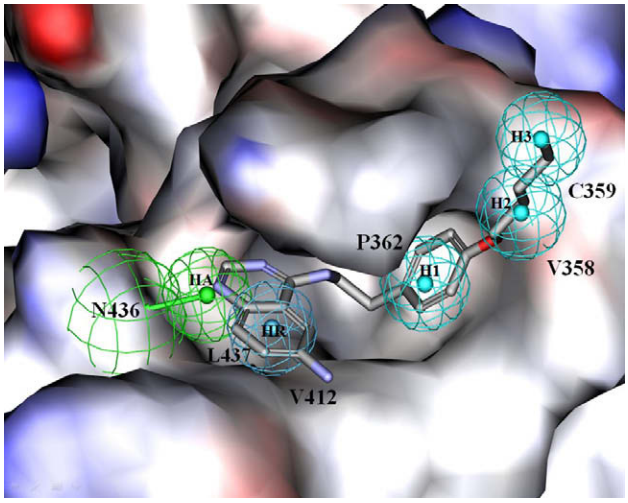

Figure 5. Pharmacophore model features of the Hypo1 with docking conformation of compound **1** mapping onto NF-κB surface from DNA binding region. Features are color-coded as follows: hydrophobic aromatic (HR), blue; hydrogen-bond acceptor (HA), green; hydrophobic (H), light blue.

Protein Data Bank (PDB code: 1VKX). The p65 subunit and DNA molecules were removed and hydrogen atoms were added. Compound **1** was docked into the p50 subunit around the DNA bind region including residues 356–368. The interpretation of herein docking results is based on this fitness function in term of relative scoring (GoldScore).[39–41] All default parameters were used for the GOLD 3.2 output from each of the genetic algorithm. The final 20 top GoldScore-ranked inhibitor-protein complexes for compound **1** were selected for the pharmacophore model Hypo1 evaluation process. The best mapping of Hypo1 and docking conformation of compound **1** around the active site surface is represented in Figure 5. It's interesting that the hydrophobic aromatic feature (HR) was correctly mapped onto hydrophobic aromatic pocket by interacting with Leu437 and Val412. Moreover, the first hydrophobic group (H1) was correctly mapped onto hydrophobic pocket (interaction with Pro362), the second hydrophobic feature (H2) was correctly mapped onto Val358, and the third hydrophobic property (H3) was probably mapped onto Cys359. Additionally, the hydrogen-bond acceptor feature (HA) has hydrogen-bond interaction with the side chain of Asn436. All evidences proved that the Hypo1 hypothesis can be mapped onto NF-κB surface correctly.

In summary, this study presents the first report for pharmacophore modeling of NF-κB inhibitors. The best pharmacophore model Hypo1, consisting of three hydrophobic groups, one hydrogen-bond acceptor, and one hydrophobic aromatic feature, was developed based on 35 known NF-κB inhibitors by using the HypoGen algorithm. This pharmacophore model was further validated by both CatScramble cross-validation and an external test set of 18 structurally diverse compounds. All results suggested that this model has accurate prediction for NF-κB inhibitors. Moreover, the pharmacophore features in Hypo1 and docking conformation were correctly matched onto NF-κB DNA binding surface. We believe that our pharmacophore model can be used for both virtual screening of novel lead compounds and chemical modification and optimization of hit compounds, therefore accelerating the discovery of new agents for the treatment of inflammatory diseases.

Acknowledgments

This project was sponsored by the National Science Council, Taiwan. (Grant No. NSC-95-2311-B-018-003) The CATALYST computation was conducted at the National Center for High Performance Computing, Taiwan.

Supplementary data

Supplementary data associated with this article can be found, in the online version, at doi:10.1016/j.bmcl.2009.08.021.

References and notes

1. Sen, R.; Baltimore, D. *Cell* **1986**, *46*, 705.
2. Beg, A. A.; Baldwin, A. S., Jr. *Genes Dev.* **1993**, *7*, 2064.
3. Baeuerle, P. A.; Henkel, T. *Annu. Rev. Immunol.* **1994**, *12*, 141.
4. Verma, I. M.; Stevenson, J. K.; Schwarz, E. M.; Van Antwerp, D.; Miyamoto, S. *Genes Dev.* **1995**, *9*, 2723.
5. Alkalay, I.; Yaron, A.; Hatzubai, A.; Orian, A.; Ciechanover, A.; Ben-Neriah, Y. *Proc. Natl. Acad. Sci. U.S.A.* **1995**, *92*, 10599.
6. Brown, K.; Gerstberger, S.; Carlson, L.; Franzoso, G.; Siebenlist, U. *Science* **1995**, *267*, 1485.
7. Scherer, D. C.; Brockman, J. A.; Chen, Z.; Maniatis, T.; Ballard, D. W. *Proc. Natl. Acad. Sci. U.S.A.* **1995**, *92*, 11259.
8. Phelps, C. B.; Sengchanthalangsy, L. L.; Malek, S.; Ghosh, G. *J. Biol. Chem.* **2000**, *275*, 24392.
9. Berkowitz, B.; Huang, D. B.; Chen-Park, F. E.; Sigler, P. B.; Ghosh, G. *J. Biol. Chem.* **2002**, *277*, 24694.
10. Schwartz, M. D.; Moore, E. E.; Moore, F. A.; Shenkar, R.; Moine, P.; Haenel, J. B.; Abraham, E. *Crit. Care Med.* **1996**, *24*, 1285.
11. Gilston, V. J.; Jones, H. W.; Soo, C. C.; Coumbe, A.; Blades, S.; Kaltschmidt, C.; Baeuerle, P. A.; Morris, C. J.; Blake, D. R.; Winyard, P. G. *Biochem. Soc. Trans.* **1997**, *25*, 518S.
12. Keates, S.; Hitti, Y. S.; Upton, M.; Kelly, C. P. *Gastroenterology* **1997**, *113*, 1099.
13. Finco, T. S.; Baldwin, A. S. *Immunity* **1995**, *3*, 263.
14. Baldwin, A. S., Jr. *Annu. Rev. Immunol.* **1996**, *14*, 649.
15. Barnes, P. J.; Karin, M. *N. Eng. J. Med.* **1997**, *336*, 1066.
16. Fiedler, M. A.; Wernke-Dollries, K.; Stark, J. M. *Am. J. Respir. Cell Mol. Biol.* **1998**, *19*, 259.
17. Nunokawa, Y.; Nakatsuka, T.; Saitoh, M.; Abe, K. World (PTC) Patent WO-0005234, 2000.
18. Tobe, M.; Isobe, Y.; Tomizawa, H.; Nagasaki, T.; Takahashi, H.; Fukazawa, T.; Hayashi, H. *Bioorg. Med. Chem.* **2003**, *11*, 383.
19. Tobe, M.; Isobe, Y.; Tomizawa, H.; Nagasaki, T.; Takahashi, H.; Hayashi, H. *Bioorg. Med. Chem.* **2003**, *11*, 3869.
20. Li, H.; Sutter, J.; Hoffmann, R. In Pharmacophore Preception, Development and Use in Drug Design; Guner, O. F., Ed.; CA, 2000; p 171.
21. CATALYST. *Version 4.11 (software package)*; Accelry: San Diego, CA; 2005, http://www.accelrys.com.
22. Debnath, A. K. *J. Med. Chem.* **2002**, *45*, 41.
23. Du, L. P.; Tsai, K. C.; Li, M. Y.; You, Q. D.; Xia, L. *Bioorg. Med. Chem. Lett.* **2004**, *14*, 4771.
24. Yang, Q.; Du, L. P.; Tsai, K. C.; Wang, X. J.; Li, M. Y.; You, Q. D. *QSAR Comb. Sci.* **2009**, *28*, 59.
25. Li, M. Y.; Tsai, K. C.; Xia, L. *Bioorg. Med. Chem. Lett.* **2005**, *15*, 657.
26. Brooks, B. R.; Bruccoleri, R. E.; Olafson, B. D.; States, D. J.; Swaninathan, S.; Karplus, M. *J. Comput. Chem.* **1983**, *4*, 187.
27. Smellie, A.; Teig, S. L.; Tobwin, P. *J. Comput. Chem.* **1995**, *16*, 171.
28. Sprague, P. W. *Perspect. Drug Discovery Des.* **1995**, *3*, 1.
29. Baumann, B.; Bohnenstengel, F.; Siegmund, D.; Wajant, H.; Weber, C.; Herr, I.; Debatin, K. M.; Proksch, P.; Wirth, T. *J. Biol. Chem.* **2002**, *47*, 44791.
30. de-Blanco, E. J.; Pandit, B.; Hu, Z.; Shi, J.; Lewis, A.; Li, P. K. *Bioorg. Med. Chem. Lett.* **2007**, *17*, 6031.
31. Xie, Y. D. S.; Thomas, C. J.; Liu, Y.; Zhang, Y. Q.; Rinderspacher, A.; Huang, W.; Gong, G.; Wyler, M.; Cayanis, E.; Aulner, N.; Többen, U.; Chung, C.; Pampou, S.; Southall, N.; Vidović, D.; Schürer, S.; Branden, L.; Davis, R. E.; Staudt, L. M.; Inglese, J.; Austin, C. P.; Landry, D. W.; Smith, D. H.; Auld, D. S. *Bioorg. Med. Chem. Lett.* **2008**, *18*, 329.
32. Muller, C. W.; Rey, F. A.; Sodeoka, M.; Verdine, G. L.; Harrison, S. C. *Nature* **1995**, *373*, 311.
33. Chen, F. E.; Huang, D. B.; Chen, Y. Q.; Ghosh, G. *Nature* **1998**, *391*, 410.
34. Prasad, A. S.; Bao, B.; Beck, F. W.; Sarkar, F. H. *J. Lab Clin. Med.* **2001**, *138*, 250.
35. Pande, V.; Sharma, R. K.; Inoue, J.; Otsuka, M.; Ramos, M. J. *J. Comput. Aided. Mol. Des.* **2003**, *17*, 825.
36. Sharma, R. K.; Otsuka, M.; Pande, V.; Inoue, J.; João Ramos, M. *Bioorg Med Chem Lett.* **2004**, *14*, 6123.
37. Pante, V.; Ramos, M. J. *Bioorg. Med. Chem. Lett.* **2005**, *15*, 4057.
38. Piccagli, L. F. E.; Borgatti, M.; Bezzerri, V.; Mancini, I.; Nicolis, E.; Dechecchi, M. C.; Lampronti, I.; Cabrini, G.; Gambari, R. *BMC Struct. Biol.* **2008**, *8*, 38.
39. GOLD is distributed by the Cambridge Crystallographic Data Center, Cambridge, UK, http://www.ccdc.ac.uk/prods/gold.html.
40. Jones, G.; Willett, P.; Glen, R. C. *J. Mol. Biol.* **1995**, *245*, 43.
41. Jones, G.; Willett, P.; Glen, R. C.; Leach, A. R.; Taylor, R. *J. Mol. Biol.* **1997**, *267*, 727.